

Supplemental Information

Controlling product selectivity in hybrid gas/liquid reactors using gas conditions, voltage, and temperature

Seung-Hoon Lee,¹ Brandon Iglesias,² Henry O. Everitt,^{3,4,*} and Jie Liu^{1,*}

¹Department of Chemistry, Duke University, Durham, North Carolina 27708, USA

²Reactwell, L.L.C. 1441 Canal Street, Lab 301 Box 5b, New Orleans, LA 70112, USA

³U.S. Army DEVCOM Army Research Laboratory-South/Rice University, 6100 Main St., Houston, TX 77005 USA

⁴Department of Physics, Duke University, Durham, North Carolina 27708, USA

*Correspondence: heveritt@duke.edu; j.liu@duke.edu

| Product | Equation | Reduction potential (V vs. RHE) |
|-----------------|-----------------------------------------------------------------------------------------------------------------|---------------------------------|
| Hydrogen | $2\text{H}_2\text{O} + 2\text{e}^- \rightarrow \text{H}_2 + 2\text{OH}^-$ | -0.828 |
| Carbon monoxide | $\text{CO}_2 + \text{H}_2\text{O} + 2\text{e}^- \rightarrow \text{CO} + 2\text{OH}^-$ | -0.932 |
| Methane | $\text{CO}_2 + 6\text{H}_2\text{O} + 8\text{e}^- \rightarrow \text{CH}_4 + 8\text{OH}^-$ | -0.695 |
| Methanol | $\text{CO}_2 + 5\text{H}_2\text{O} + 6\text{e}^- \rightarrow \text{CH}_3\text{OH} + 6\text{OH}^-$ | -0.812 |
| Formic acid | $\text{CO}_2 + \text{H}_2\text{O} + 2\text{e}^- \rightarrow \text{HCOO}^- + \text{OH}^-$ | -0.639 |
| Ethylene | $2\text{CO}_2 + 8\text{H}_2\text{O} + 12\text{e}^- \rightarrow \text{C}_2\text{H}_4 + 12\text{OH}^-$ | -0.743 |
| Ethanol | $2\text{CO}_2 + 9\text{H}_2\text{O} + 12\text{e}^- \rightarrow \text{CH}_3\text{CH}_2\text{OH} + 12\text{OH}^-$ | -0.744 |
| Acetic acid | $2\text{CO}_2 + 5\text{H}_2\text{O} + 8\text{e}^- \rightarrow \text{CH}_3\text{COO}^- + 7\text{OH}^-$ | -0.653 |

Table S1. Calculated standard reduction potential values in V vs. reversible hydrogen electrode (RHE) for various CO₂RR products from reference.¹

Photograph of the hybrid gas/liquid reactor

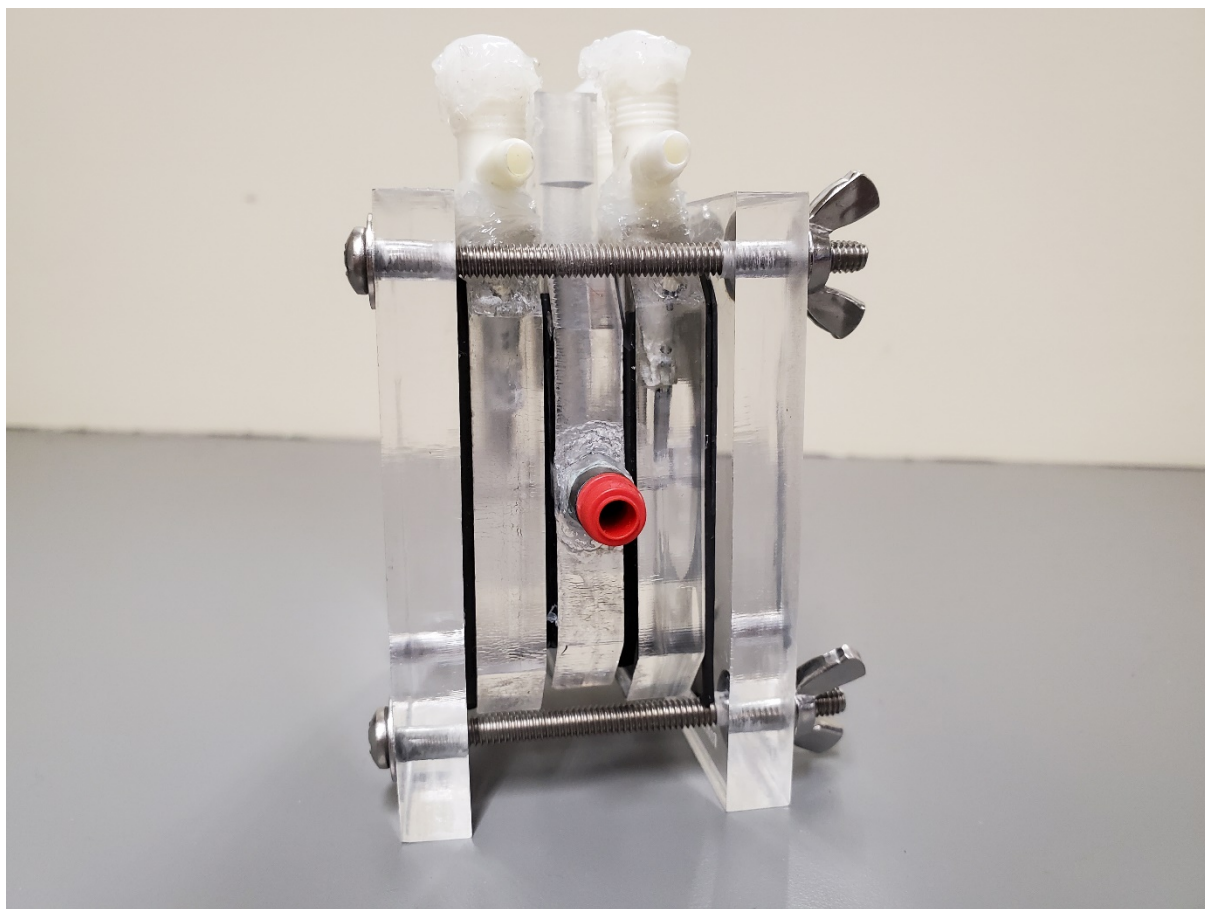


Fig. S0. A photograph of the hybrid gas/liquid reactor.

Hybrid reactor with water bath for controlling electrolyte temperature

The CO₂RR occurs at the three-phase (gas-catalyst-electrolyte) boundary of the gas-facing side of the cathode,^{2,3} while the oxygen evolution reaction (OER) occurs at the anode.⁴ Some of the products will be produced on the fully wetted catalyst facing the electrolyte, while others will be produced on the drier catalyst facing the gas chamber (Fig. 1B). All the data are presented with respect to the reversible hydrogen electrode (RHE) scale. The anode was a Pt mesh, and an anion exchange membrane (FAA-3-pk-75, FuelCell store) was used. The 0.1 ml/min flow of the 1M KOH electrolyte supplied to the reference and anodic cells was controlled by a syringe pump. Although CO₂ was bubbled through the electrolyte, it remained strongly basic (see pH measurement).

For the gas supply, the flow of dry CO₂ gas was regulated by a CO₂ mass-controller feeding the inlet of the reactor. For the humidified CO₂ condition, a water bottle was placed between the two through which the CO₂ gas bubbled. The volume of empty space in the water bottle was about 0.24 L, and CO₂ gas was bubbled with a flow rate of >30 ml/min for at least 30 minutes. Since the outlet of the reactor was open during the CO₂ bubbling process, the total pressure was 1 atm, and vapor pressure of water at 22°C as 0.026 atm. Thus, the percentage of water vapor in the CO₂ gas was ~2.7%.

To control the electrolyte temperature, the reactor was placed in a water bath sitting on a hot plate. The electrolyte temperature was measured by an epoxy-coated thermocouple (TC-PVC-E-24-180, Omega) attached to the catalyst in the reference cell and monitored by a temperature data logger (RDXL6SD, Omega). Experiments began after the electrolyte temperature reached the target temperature and the electrolyte temperature remained constant. (see Fig. S1-2).

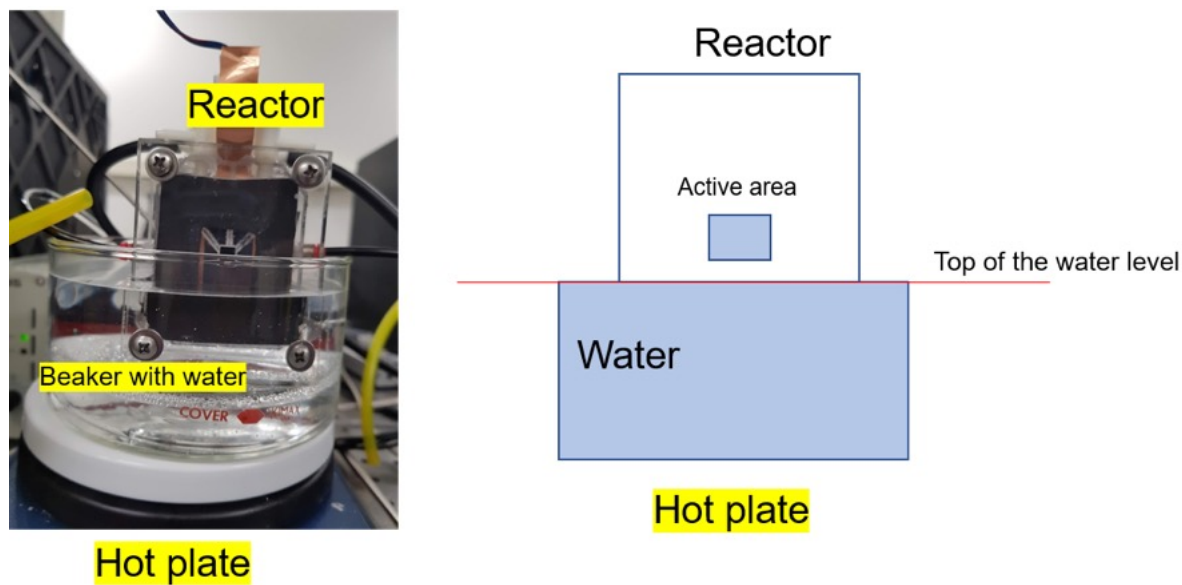
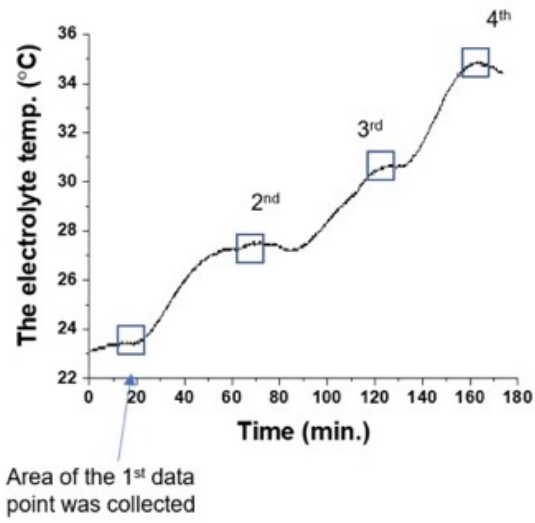


Fig. S1. Photograph (left) and scheme (right) showing how the electrolyte temperature was controlled with a hot plate. For temperature monitoring, a thermocouple was inserted through the reference cell and the endpoint of the thermocouple slightly touched the catalyst.

Temporal evolution of electrolyte temperature

The desired temperature was set on the hot plate. After the electrolyte temperature in the reactor reached that temperature and remained constant (Fig. S2), a potential was applied and data was collected.



Zoomed graph

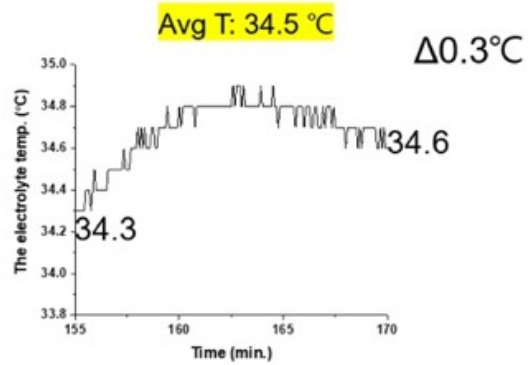
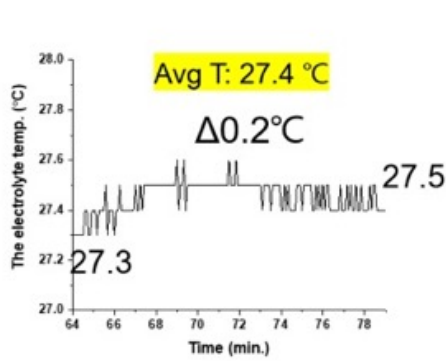
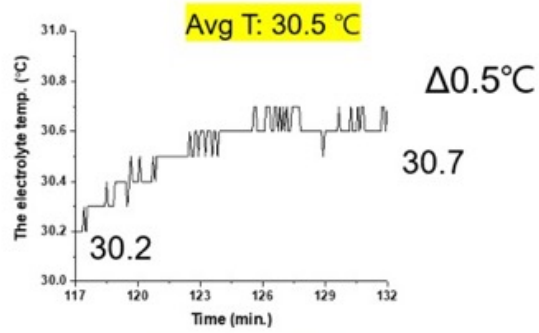
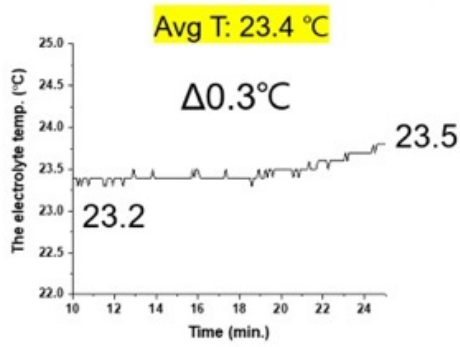


Fig. S2. Electrolyte temperature vs. time graph.

Preparation of cathode and catalyst

The gas-diffusion electrode (GDE) cathode used here was composed of randomly oriented carbon fibers covered by a dense nanotextured array of carbon nanospikes (CNSs) approximately 50–80 nm in length (Fig. S3). Each nanospike consisted of layers of puckered carbon, ending in a ~2 nm wide curled tip.⁵ A copper on this CNS-cathode showed over 60% CO₂RR conversion efficiency toward ethanol in a liquid-phase experiment.⁵

To prevent leakage, PTFE was applied to the GDE cathode. A commercial PTFE dispersion (College Station, Texas, USA) with 60wt% was diluted with deionized water to produce a 10wt% PTFE dispersion solution. The CNS cathode was immersed into this 10wt% PTFE dispersion for less than 1 minute, then heated in a furnace under 5% H₂ balance Ar environment at 350°C for 30 minutes. These PTFE coating steps were repeated three times.

Next, the liquid-facing side of the GDE was coated with a CO₂RR catalyst using an ink composed of 0.1 g of commercial copper nanoparticles (774081-5G, Sigma Aldrich) dispersed in a mixture of methanol, a 0.075g solution of Nafion (527084-25 ML, Sigma Aldrich), and 0.01g of PTFE particles (430935-100G, Sigma Aldrich). The mixture was sonicated for >1 hour to produce the Cu ink that was painted on the PTFE-treated cathode using an air-brush. Before spray-casting of the Cu ink, ~80 µl of 10% PTFE-dispersion was drop cast to the center area of the cathode to avoid any PTFE damage from the methanol. Then, the Cu ink was painted on the PTFE-treated cathode using an air-brush after the 80 µl of the 10% PTFE-dispersion was dried. After this, the sample was heated in a furnace under 5% H₂ balance with Ar at 350°C for 30 minutes. Lastly, one additional 3% PTFE-coating was applied on just the gas side. The amount of copper nanoparticles (NPs) in the center area of the cathode (~1.5 cm × 1.5 cm) was about 55 mg/cm². The active area of the catalyst facing the gas-chamber was ~ 5 mm × 5 mm.

Without the PTFE coating on the both GDE and catalyst, the electrolyte flooded through the GDE, and the current began fluctuating unstably within an hour (Fig. S4). The lack of flooding and the stable current for > 1 hour in the measurements reported here confirm that PTFE created a good hydrophobic environment for the GDE catalyst.

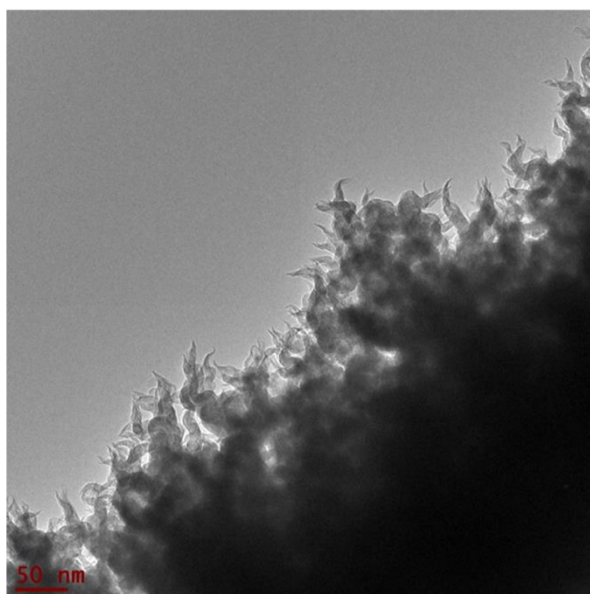


Fig. S3. Transmission electron microscope image of a carbon nanospike on a carbon fiber.

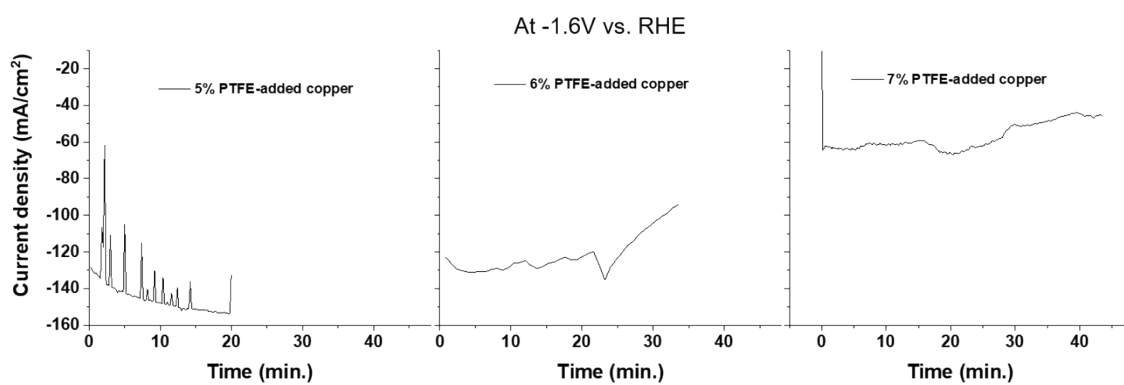


Fig. S4. The total current density at a low PTFE percentage in the catalyst layer. Each

percentage represents the PTFE amount of copper.

Measurements

All electrochemical measurements were performed using a WaveNow Potentiostat (PINE research Instrumentation, Durham, North Carolina, USA). The reacted electrolyte was collected for 15 min through an outlet of the reference cell. Then, a small part of the reacted electrolyte, 545 μl , was mixed with 50 μl of D_2O (161882-25G, Sigma Aldrich) and 5 μl of dimethyl Sulfoxide (DMSO, 10 mM as an internal standard, >99.7%, Fisher)] for the NMR measurements (Bruker 500 ICON NMR). The molar concentration of each liquid product (C_x)

was calculated using
$$C_x = \frac{I_{liquid}}{I_{DMSO}} \times \frac{N_{DMSO}}{N_{liquid}} \times C_{DMSO}$$
, where I , N , and C_i are the integral area of the NMR signal, the number of protons, and the concentration of the compound of interest ($i =$ liquid product x or calibrant DMSO), respectively. Then, the production rate of liquid products was calculated as the ratio of C_x to the collection time and active areas of the catalyst.

The gaseous products were analyzed by a quadrupole mass spectrometer (Hiden, HPR-20, Warrington, United Kingdom) equipped with a Faraday cup detector. An outlet of the cathodic cell was coupled to a sampling point of the mass spectrometer. In all experiments, a bypass Ar flow with 10 ml/min was directly delivered to the mass-spec with CO_2 gas to maintain the total flow rate as 20 ml/min. A background signal was collected with the carrier gases for at least 10-30 minutes before starting an experiment.

Each mass spectrometer signal was calibrated using calibration gases (Gasco, Inc.).

Then, the amount of gas product (G_x) was calculated using
$$G_x = p_{avg} t_{sample} \frac{\Phi}{22400}$$
, where G_x is in moles, t_{sample} is the sampling time in minutes, and Φ is total flow rate in ml/min. We measured three gas products at $m/z = 2$ (H_2), 15 (CH_4), and 27 (C_2H_4). To calculate the averaged fractional pressure p_{avg} (unitless), the ratio of the measured mass spec signals for each gas product and the Ar reference (e.g. averaged H_2 signal / averaged Ar signal) were averaged over 15 minutes.

This averaged signal ratio value was inserted into the calibration curve for each gas to ascertain the averaged fractional pressure value p_{avg} for the product. (The calibration curve of each gas was obtained by a standard calibration gas.) Then, the production rate of gas products was calculated using the same ratio described above for gas products. The Faradaic efficiency of each product is calculated using the procedure discussed below.

Current stability

For low PTFE film coverage of the carbon fibers and no PTFE particles, we obtained a high total current density ($>100 \text{ mA/cm}^2$), but flooding usually happened within an hour, after which the total current fluctuated and was unstable. The flooding inhibits access of CO_2 gas to the catalyst, so it caused an unstable current. The main reason for the flooding is the reduced hydrophobicity (1) by the spray-casting of the Cu ink composed of an organic solvent without PTFE particles on the cathode, (2) formation of liquid products such as ethanol, (3) salt precipitation during operation, and (4) an application of the large cathodic bias.⁶ To maintain the PTFE layer and make a current stable for > 1 hour, we added the 10% PTFE particles to the Cu ink and tried a 3% PTFE coating on the cathode after the spray-casting. In addition, a low bias ($-1.6\text{V} \rightarrow -0.8\text{V}$) was applied to minimize the PTFE damage. These approaches yielded a stable current density over time, even though the total current density was lower.

Comparison of methane and ethylene production

Ethylene calibration has been reported in an earlier paper.⁷ By subtracting out the $m/z=15$ contributions from ethylene (since ethylene has a splitting signal at $m/z=15$) when calculating the methane signal, we find that methane and ethylene behave almost identically

(Fig. S5). The differences are small, the amounts of products are very similar, and the trends are identical.

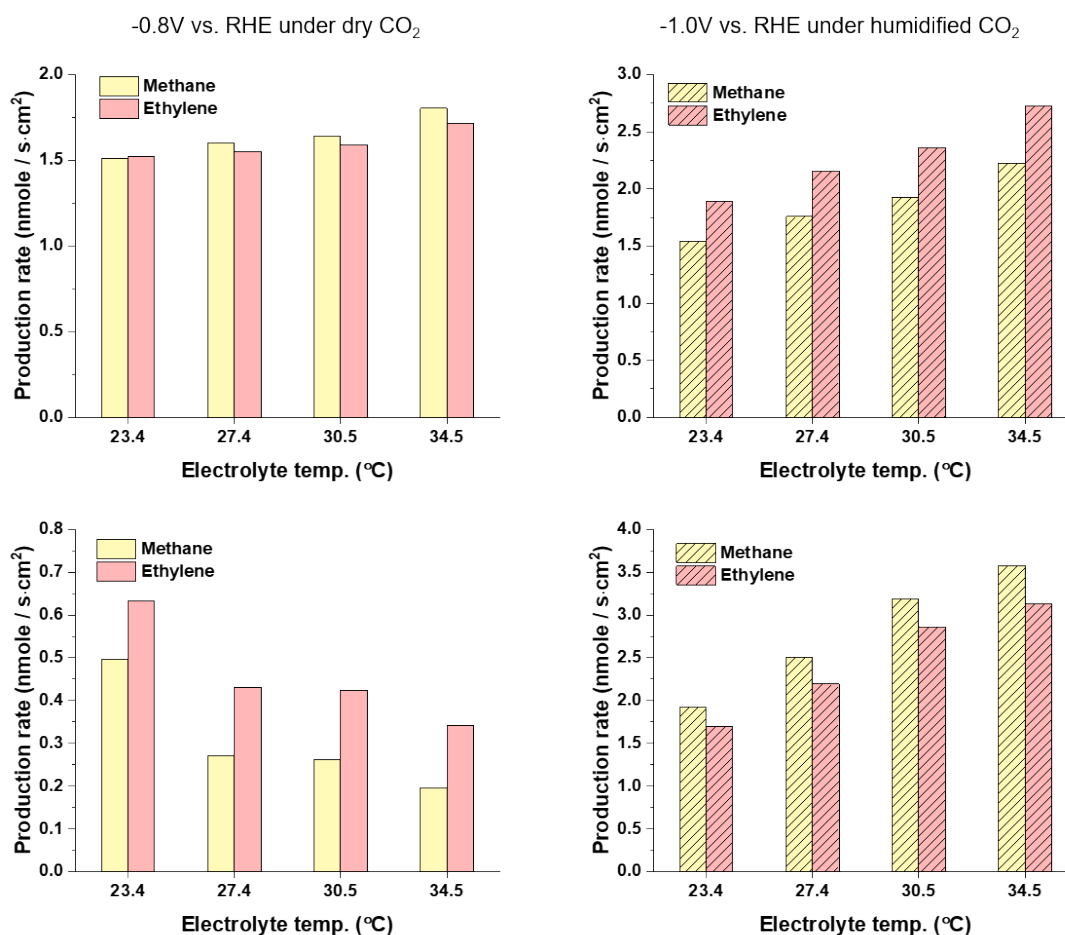


Fig. S5. Production rate of methane and ethylene at two applied potentials under dry and humidified CO₂ conditions.

Faradaic efficiency of each product

Faradaic efficiency (FE) of liquid products (Fig. S6) was calculated using the following formula:

$$FE = \frac{q_1}{q_{tot}} = f \times c_x \times V \times z_1 / q_{tot} \times 100, \quad (1)$$

where f , V , z_1 , q_{tot} are the faraday constant (C/mol), the volume of the reacted electrolyte (liters), the number of electrons to produce the liquid product, and the total charge ($q_{tot} = \int Idt$), respectively. Liquid peaks were calibrated with pure 1-propanol (99+%, Acros), acetic acid (>99%, Sigma-Aldrich), formic acid (> 95%, Sigma-Aldrich), and ethanol (99.5%, anhydrous, VWR), respectively. For example, 5 μ l of each pure liquid was added to the mixture of 540 μ l of pure 1M KOH and 50 μ l of D₂O for the calibration.

The FE of the gas products (Fig. S6) was calculated using the following equation:

$$FE = \frac{q_1 (output)}{q_{tot} (input)} = f \times G_x \times z_g / q_{tot} \times 100, \quad (2)$$

where z_g is the number of electrons to produce a gas product, and q_{tot} is the total charge ($\int Idt$).

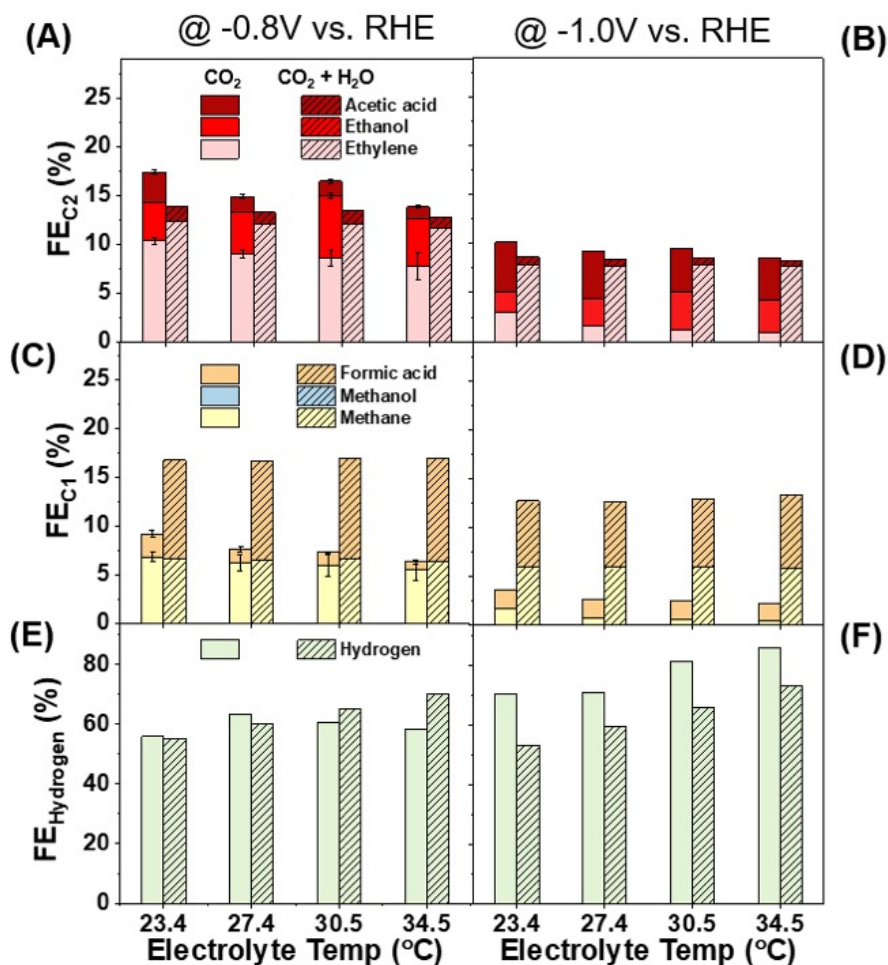


Fig. S6. FE of each product at all conditions.

pH measurement after CO₂ bubbling

The 1M KOH electrolyte had CO₂-bubbled through it. Before CO₂ bubbling, the pH of 1M KOH was 13.91, and it became 12.66 after the CO₂ bubbling for 1 hour. The pH is measured by a glass membrane electrode type (S20 sevenEasy, METTER LLC, Ohio, USA) after the calibration with four different pH buffer solutions (a pH of 4.0, 7.0, 10.01, and 1.68).

The OH⁻ change after CO₂ bubbling is $\Delta[OH^-] = 10^{-0.09} - 10^{-1.34} = 0.767 M$.

Carbonate production

The reaction of KOH and CO₂ is



A loss of 0.767M KOH corresponds to a formation of 0.384M CO_3^{-2} .

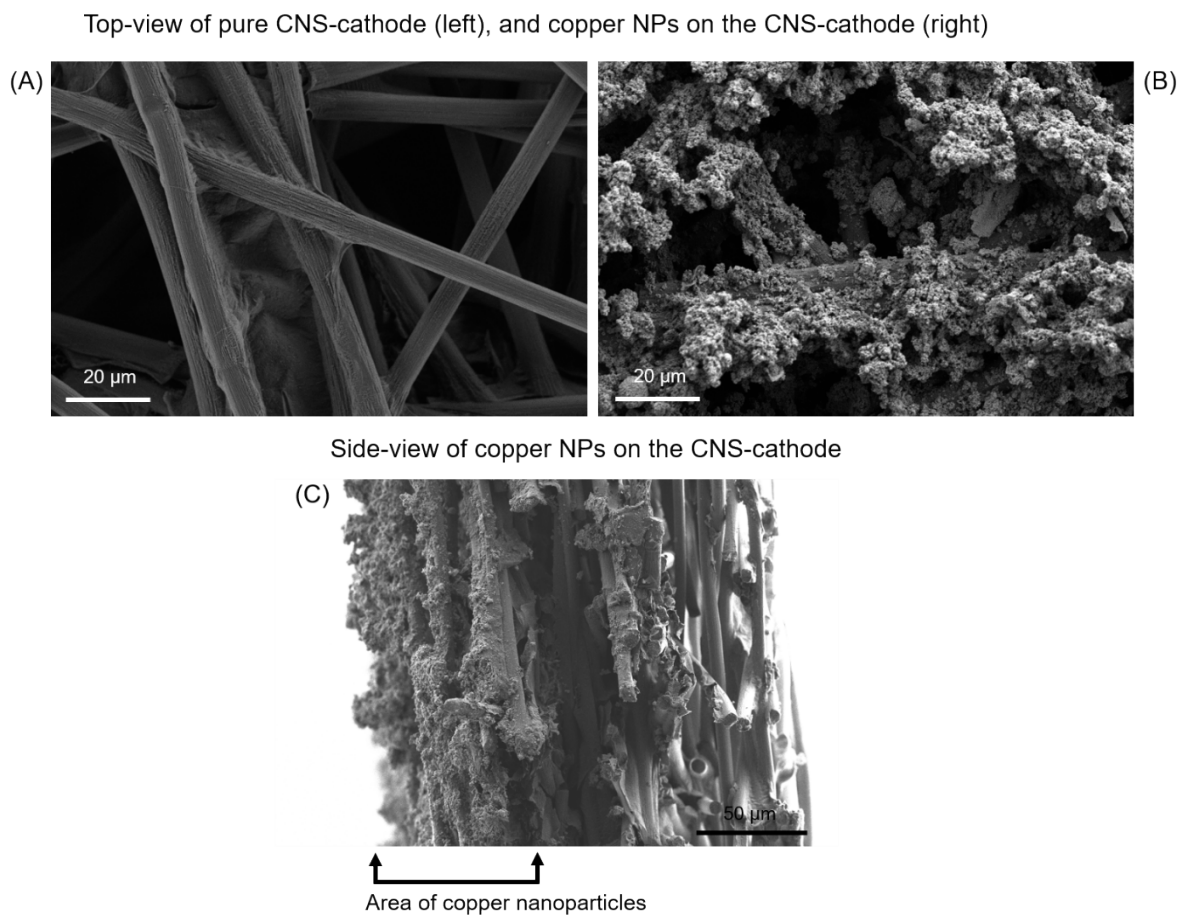


Figure S7. Top and side-view SEM images of pure CNS-cathode (A) and copper NPs on the CNS cathode (B and C). A CNS cathode is composed of carbon fibers and copper nanoparticles were deposited on this cathode.

References

- 1 L. Fan, C. Xia, F. Yang, J. Wang, H. Wang and Y. Lu, *Sci. Adv.*, 2020, **6**, eaay3111.
- 2 M. Jouny, W. Luc and F. Jiao, *Nat. Catal.*, 2018, **1**, 748-755.
- 3 L.-C. Weng, A. T. Bell and A. Z. Weber, *Phys. Chem. Chem. Phys.*, 2018, **20**, 16973-16984.
- 4 M. B. Ross, P. De Luna, Y. Li, C.-T. Dinh, D. Kim, P. Yang and E. H. Sargent, *Nat. Catal.*, 2019, **2**, 648-658.
- 5 Y. Song, R. Peng, D. K. Hensley, P. V. Bonnesen, L. Liang, Z. Wu, H. M. Meyer III, M. Chi, C. Ma, B. G. Sumpter and A. J. Rondinone, *ChemistrySelect*, 2016, **1**, 6055-6061.
- 6 K. Yang, R. Kas, W. A. Smith and T. Burdyny, *ACS Energy Lett.*, 2021, **6**, 33-40.

7 S.-H. Lee, Y. Song, B. Iglesias, H. O. Everitt and J. Liu, *ACS Appl. Energy Mater.*, 2022, **5**, 9309-9314.